MCB
Journals.ASM.org

Patched-1 Proapoptotic Activity Is Downregulated by Modification of K1413 by the E3 Ubiquitin-Protein Ligase Itchy Homolog

Xiaole L. Chen,[a] Pilar Chinchilla,[a]* Joanna Fombonne,[b] Lan Ho,[a] Catherine Guix,[b] James H. Keen,[a,c] Patrick Mehlen,[b] Natalia A. Riobo[a,c]

Department of Biochemistry and Molecular Biology, Thomas Jefferson University, Philadelphia, Pennsylvania, USA[a]; Apoptosis, Cancer and Development Laboratory-Equipe Labellisée la Ligue, LabEx DEVweCAN, Centre de Cancérologie de Lyon, INSERM U1052-CNRS UMR5286, Université de Lyon, Centre Léon Bérard, Lyon, France[b]; Kimmel Cancer Center, Thomas Jefferson University, Philadelphia, Pennsylvania, USA[c]

The Hedgehog (Hh) receptor Patched-1 (PTCH1) opposes the activation of Gli transcription factors and induces cell death through a Gli-independent pathway. Here, we report that the C-terminal domain (CTD) of PTCH1 interacts with and is ubiquitylated on K1413 by the E3 ubiquitin-protein ligase Itchy homolog (Itch), a Nedd4 family member. Itch induces the ubiquitylation of K1413, the reduction of PTCH1 levels at the plasma membrane, and degradation, activating Gli transcriptional activity in the absence of Hh ligands. Silencing of Itch stabilizes PTCH1 and increases its level of retention at the plasma membrane. Itch is the preferential PTCH1 E3 ligase in the absence of Hh ligands, since of the other seven Nedd4 family members, only WW domain-containing protein 2 (WWP2) showed a minor redundant role. Like Itch depletion, mutation of the ubiquitylation site (K1314R) resulted in the accumulation of PTCH1 at the plasma membrane, prolongation of its half-life, and increased cell death by hyperactivation of caspase-9. Remarkably, Itch is the main determinant of PTCH1 stability under resting conditions but not in response to Sonic Hedgehog. In conclusion, our findings reveal that Itch is a key regulator of ligand-independent Gli activation and noncanonical Hh signaling by the governance of basal PTCH1 internalization and degradation.

The Hedgehog (Hh) signaling pathway has essential roles in embryonic development, tissue homeostasis, and tumorigenesis. The pathway is activated by binding of any of the three mammalian Hh isoforms, Sonic Hedgehog (Shh), Indian Hedgehog (Ihh), or Desert Hedgehog (Dhh), to the 12-transmembrane protein Patched-1 (PTCH1). The mammalian genome encodes a second PTCH homologue, PTCH2, with tissue-restricted functions that shares an overall 54% amino acid sequence identity with PTCH1 (1). The most divergent regions between these proteins are the intracellular C-terminal domain (CTD) and the central intracellular loop. PTCH1 is an atypical receptor, in that it does not couple to heterotrimeric G proteins and lacks a kinase domain. Instead, PTCH1 has a sterol-sensing domain (SSD) resembling bacterial permeases that pump small hydrophobic compounds, and mutations in residues that are critical for its function in bacteria abolish PTCH1's activity (2). In the absence of Hh ligands, PTCH1 actively represses the 7-transmembrane protein Smoothened (SMO) by a yet unknown mechanism. Hh binding to PTCH1 inhibits its catalytic activity and promotes its internalization, leading to the derepression of SMO. SMO-mediated signaling is complex and involves trafficking to the primary cilium, activation of heterotrimeric G-inhibitory proteins (G_i proteins), and interaction with the scaffolding protein Ecv2 (3). Activation of SMO regulates a number of protein kinases to prevent the degradation of and fully activate the Gli family of transcription factors in the so-called canonical Hh pathway.

PTCH1 is a tumor suppressor protein, as revealed by frequent loss-of-function mutations and deletions in basal cell carcinomas, medulloblastoma, and rhabdomyosarcoma (4–9). PTCH2-deficient mice show no obvious birth defects and are cancer prone only on a PTCH1 heterozygous background (10).

Interestingly, PTCH1 not only acts to repress SMO but also has a distinguishable function as a proapoptotic dependence receptor (11, 12). Dependence receptors induce apoptosis when they are not occupied by a ligand (11–13). Hh binding to PTCH1 inhibits this apoptotic activity, apparently via a type I noncanonical signaling pathway, independently of SMO- and Gli-dependent transcription (2, 11, 14–16). In the absence of any of the three Hh ligands, PTCH1 induces apoptosis through its intracellular CTD, which is largely dispensable for canonical Hh signaling (11, 16, 17). The CTD is proteolyzed at D1392 by caspase, exposing a binding site for the scaffolding proteins DRAL and TUCAN1, which recruit caspase-9 (12). Aggregation and activation of caspase-9 by ubiquitylation amplify the proteolytic cascade, which culminates with the irreversible commitment to cell death when the executioner caspases, caspases 3 and 7, are fully activated (12).

Ubiquitylation, the posttranslational addition of one or more ubiquitin (Ub) polypeptides to a protein, was initially found to label proteins for proteasome-mediated degradation. Later, ubiquitylation was shown to affect membrane receptor endocytosis, intravesicular sorting, and lysosomal degradation (18). Ubiquitin conjugation is an ATP-dependent reaction that involves the sequential activation of three enzymes, ubiquitin-activating enzyme E1, ubiquitin-conjugating enzyme E2, and ubiquitin ligase E3, which determine substrate specificity. More than 600 different E3 ligases have been found (19). Many E3 ligases have either oncogene or tumor suppressor functions. E3 ligases can be classified

Received 24 July 2014 Returned for modification 27 July 2014
Accepted 28 July 2014
Published ahead of print 4 August 2014
Address correspondence to Natalia A. Riobo, natalia.riobo@jefferson.edu.
* Present address: Pilar Chinchilla, Institute of Pharmacology, University of Marburg, Marburg, Germany.

doi:10.1128/MCB.00960-14

into two families: the RING (the really interesting new gene) family and the HECT (homologous to E6-AP C terminus) family. The HECT family contains 28 members and can be subdivided into 3 groups: Nedd4 (the neuronal precursor cell expressed developmentally downregulated 4), HERC, and other HECTs (20, 21). There are nine Nedd4-like E3 ligases, including Itchy homolog/atrophin-interacting protein-4 (Itch/AIP4) and WW domain-containing protein 2 (WWP2), which contain an N-terminal C2 domain, two to four WW domains, and a C-terminal HECT domain. Accumulating evidence has linked Nedd4-family E3 ligases to cancer through internalization and/or degradation of growth and metastasis regulatory proteins, such as p53, p63, PTEN, CXCR4, and transforming growth factor β (22–24).

Searching for proteins that could modulate PTCH1 apoptotic function by mass spectrometry, we found that the Itch and WWP2 ubiquitin E3 ligases physically associate with the CTD of PTCH1 but not with PTCH2. We present evidence that PTCH1 is ubiquitylated at K1413 in the C-terminal domain by Itch and, to a lesser extent, by WWP2, internalized, and targeted for proteasomal degradation. Overexpression of Itch is sufficient to stimulate Gli transcriptional activity. Addition of Shh stimulates K1413 ubiquitination, reduces the level of PTCH1 at the plasma membrane, and promotes its degradation. K1413 ubiquitylation inhibits PTCH1 proapoptotic activity, presumably by reducing the plasma membrane levels of PTCH1. Therefore, Itch is a critical regulator of Hh signaling by controlling the level of the tumor suppressor PTCH1.

MATERIALS AND METHODS

Reagents. Recombinant Shh was synthesized and purified as described previously (25). KAAD-cyclopamine 3-keto-*N*-(aminoethyl-aminocaproyl-dihydrocinnamoyl)cyclopamine] and MG132 were purchased from EMD Biosciences (Madison, WI). Chloroquine and ammonium chloride were purchased from Sigma-Aldrich (St. Louis, MO). Lactacystin and Z-VAD-FMK were from Enzo Life Sciences (Farmingdale, NY). Antihemagglutinin (anti-HA; 9B11), anti-myc (9B11), anti-PTCH1 (C53A3), and anti-Ub (P4D1) antibodies were from Cell Signaling Technology (Danvers, MA); anti-Itch/AIP4 and anti-β-actin were from Sigma-Aldrich (St. Louis, MO); anti-WWP2 was from Bethyl (Montgomery, TX); anti-PTCH1 G19, cycloheximide, and secondary anti-rabbit horseradish peroxidase (HRP)-conjugated and anti-mouse HRP-conjugated antibodies were from Santa Cruz Biotechnology (Santa Cruz, CA); and secondary anti-rabbit and anti-mouse Alexa Fluor-conjugated antibodies were from Life Technologies (Grand Island, NY).

Plasmids and adenoviral vectors. HA-tagged PTCH1 (PTCH1-HA) and the HA-tagged PTCH1 D1392N mutant were already described (11). Enhanced green fluorescent protein (eGFP)-tagged PITCH1 (PTCH1-eGFP) was a generous gift from Kazuaki Nagao (National Center for Child Health and Development, Japan). K1413R mutations were created by site-directed mutagenesis of full-length PTCH1 using a QuikChange kit (Agilent Technologies, Santa Clara, CA). Itch, catalytically inactive Itch [Itch(CA)], WWP2, and catalytically inactive WWP2 [WWP2(CA)] were generous gifts from Mark von Zastrow and Adriano Marchese (University of California, San Francisco). Plasmid DNA (pcDNA) encoding PTCH2 (pcDNA-PTCH2) was a generous gift from Peter Zaphiropoulos (Karolinska Institutet, Sweden). Green fluorescent protein (GFP)-tagged PTCH1 CTD (GFP-CTD1) and GFP-taged PTCH2 CTD (GFP-CTD2) were constructed by PCR amplification and subcloned into pAcGFP-Mem (Clontech, Mountain View, CA). CTD1 and the K1413R (KR) mutant of CTD1 [CTD1(KR)] with an HA epitope tag were subcloned into the pcDNA3.1+ vector (Life Technologies). pShuttle-PTCH1-IRES-eGFP and pShuttle-PTCH2-IRES-eGFP were generated by subcloning. Adenoviruses were generated with an AdEasy kit (Agilent Technologies) and amplified in AD-HEK293T cells, and the titer was determined using an AdEasy viral titer kit (Agilent Technologies).

Cell culture and transgene expression. HEK293 cells, 293T COS-1 cells, $Ptc1^{-/-}$ mouse embryonic fibroblast (MEFs) (from Matthew Scott, Stanford University), and $SMO^{-/-}$ MEFs (from James Chen, Stanford University) were cultured in Dulbecco's modified Eagle medium with 10% fetal bovine serum (Life Technologies), 100 U/ml penicillin, and 100 μg/ml streptomycin. NIH 3T3 cells were cultured in Dulbecco's modified Eagle medium containing 10% (vol/vol) calf serum (Colorado Serum Co.), 100 U/ml penicillin, and 100 μg/ml streptomycin. All cells were maintained in a humidified 37°C incubator at 5% CO_2.

Plasmids were introduced into HEK293T cells, COS-1 cells, and $Ptc1^{-/-}$ MEFs using the Lipofectamine reagent (Life Technologies) and into NIH 3T3 cells using the Fugene HD reagent (Roche, Indianapolis, IN), following the manufacturers' instruction. Adenoviral infections were carried out at a multiplicity of infection (MOI) of 400 for 24 h.

RNA interference. Control small interfering RNA (siRNA; catalog number 4390843), Itch siRNA-1 (sense sequence, 5′-GGAACUGCUGCAUUAGAUATT-3′; antisense sequence, 5′-UACCAUUCUGAUGUAUUCCTC-3′), Itch siRNA-2 (sense, 5′-GGAACUGCUGCAUUAGAUATT-3′; antisense, 5′-UAUCUAAUGCAGCAGUUCCCA-3′), WWP2 siRNA-1 (5′-CAGGAUGGGAGAUGAAAUAUU-3′) (22), and WWP2 siRNA-2 (catalog number HSS174069; Invitrogen) were purchased from Life Technologies (Grand Island, NY). Transfection was performed with 5 nM siRNA using the HiPerFect transfection reagent (Qiagen, Valencia, CA) according to the manufacturer's protocol, and experiments were done after 72 h.

IP. For immunoprecipitation (IP) or coimmunoprecipitation (co-IP), cells were lysed in IP lysis buffer (20 mM Tris, pH 7.5, 150 mM NaCl, 1% NP-40, 2 mM EDTA, protease inhibitors [Roche Complete Mini]) for 30 min at 4°C. Lysates were cleared by centrifugation at 4°C. Antibodies were added as recommended by the manufacturer for 2 h, followed by incubation with protein A-Dynabeads (Life Technologies) for 1 h at 4°C. After three washes with IP lysis buffer, proteins were eluted in Laemmli sample buffer for Western blotting. For IP experiments under denaturing conditions, cells were lysed in denaturing buffer (20 mM Tris-HCl, pH 7.5, 1% SDS), followed by sonication and 1:10 dilution in IP buffer containing 10 mM *N*-ethylmaleimide.

Caspase-9 activity assay on immunoprecipitated PTCH1. Cells that had been transfected with empty vector, PTCH1-HA, or a construct consisting of PTCH1-HA carrying CTD(KR) [PTCH1(KR)-HA] with the JetPRIME reagent (Polyplus, France) according to the manufacturer's instructions were plated in 6-well plates at 1.5×10^5 cells/well. Shh-conditioned medium, the supernatant of HEK293T cells expressing muristerone A-inducible Shh (HEK293T-EcRShh), was added at the time of transfection, as previously described (11). Cells were harvested 48 h later and lysed in 50 mM HEPES, pH 7.6, 150 mM NaCl, 5 mM EDTA, and 1% NP-40 in the presence of protease inhibitors (Roche). For immunoprecipitation of PTCH1, lysates were incubated for 1 h at 4°C with 1 μg anti-PTCH1 G19 antibody (Santa Cruz) and protein A-Sepharose (Sigma-Aldrich). The beads were washed four times in 50 mM HEPES, pH 7.6, 150 mM NaCl, 5 mM EDTA. Caspase-9 activity was measured directly on the beads using a Caspase-Glo 9 assay kit (Promega, Madison, WI) according to the manufacturer's instructions.

To confirm that the amounts of immunoprecipitated PTCH1 and PTCH1(KR) were equal, the beads were subsequently boiled in Laemmli sample buffer and analyzed by Western blotting with anti-PTCH1 G19 antibody (1:1,000 dilution).

Mass spectrometry. Samples from the co-IP were subjected to SDS-PAGE and stained with Coomassie G250 (GelCode blue stain; Thermo Scientific, Waltham, MA). The protein bands were excised and sent to the Thomas Jefferson University Proteomics Facility for tandem mass spectrometry. Peptide analysis and protein identification were done using the Mascot program.

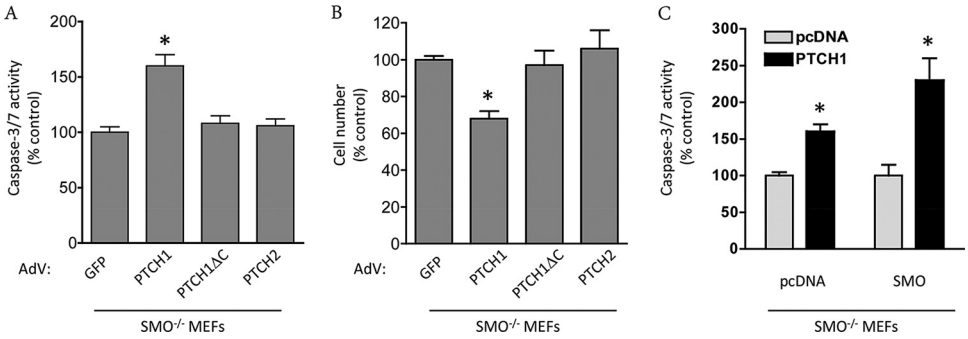

FIG 1 PTCH1 induces apoptosis in an SMO-independent manner. (A) SMO-deficient MEFs were infected with bicistronic adenoviruses (AdV) carrying GFP alone or GFP plus PTCH1, PTCH1 with a CTD deletion (PTCH1ΔC), or PTCH2 at an MOI of 400, and 24 h later the cells were lysed and caspase-3/7 activity was determined by luminescence. (B) Same as panel A, but the viable cell number was quantified by trypan blue reduction. (C) SMO-deficient MEFs were stably transfected with empty vector (pcDNA) or with pcDNA carrying SMO (SMO). After antibiotic selection of positive clones, cells were infected with adenovirus carrying GFP or adenovirus carrying PTCH1, as described for panel A, and caspase-3/7 activity was determined 24 h later. All experiments were repeated 3 times, and results are expressed as means ± SEMs. *, $P < 0.01$.

Immunofluorescence. COS-1 cells were seeded and transfected on Lab-Tek II chamber slides. After the period of time indicated below, cells were fixed in 4% formaldehyde (Ted Pella, Inc.) for 15 min, washed three times with phosphate-buffered saline (PBS), and blocked in PBS containing 5% goat serum and 0.1% saponin for 1 h at room temperature. Primary antibodies were diluted in antibody solution (PBS, 1% bovine serum albumin, 0.1% saponin) and incubated at 4°C overnight. After washing three times with PBS, secondary antibodies conjugated with Alexa Fluor dyes (Life Technologies) were added for 1 h at room temperature. After a final PBS wash, the slides were mounted with Prolong Gold antifade reagent (Life Technologies). Pictures were taken on a Zeiss LSM510 Meta confocal laser scanning microscope (Kimmel Cancer Center Imaging Facility) or a Nikon Eclipse E800 epifluorescence microscope and analyzed by use of the LSM image browser or Nikon NIS Elements BR (version 3.0) software.

Luciferase assay. Cells were seeded in 24-well plates and transfected on the following day when they were at ~70% confluence. PTCH1 variants or empty vector, p8XGBS-Luc, and pRL-TK were transfected at a ratio of 4:1:0.1 using the Fugene HD reagent according to the manufacturer's protocol. When cells reached 100% confluence, typically between 24 and 48 h after transfection, the medium was changed to 0.5% serum for an additional 24 h. Luciferase activity was determined with a dual-luciferase reporter assay system (Promega) in a Promega Glomax 20/20 luminometer following the manufacturer's directions.

Plasma membrane protein biotinylation. The plasma membrane fraction was isolated as suggested by the instructions accompanying the Pierce cell surface protein isolation kit (Thermo Scientific), with modifications made to better solubilize membrane proteins. Briefly, at 16 h after transfection, the plasma membrane of HEK293T cells was labeled with biotin. The cells were lysed with lysis buffer (25 mM Tris, pH 7.2, 150 mM NaCl, 1% SDS, 5% NP-40, 1% sodium deoxycholate, and 1 mM EDTA supplemented with protease inhibitors). After sonication, the cell lysates were diluted 10 times with wash buffer (25 mM Tris, pH 7.2, 150 mM NaCl, 1% NP-40, 0.1% SDS, 1% sodium deoxycholate, 1 mM EDTA). Biotinylated proteins were separated using NeutrAvidin agarose and analyzed by Western blotting.

Quantification of cell death. Cell death was analyzed 48 h after transfection using trypan blue staining procedures (11). At 24 h after transfection, caspase-3/7 activity was measured with a Caspase-Glo 3/7 assay kit (Promega) following the manufacturer's instructions.

Statistics. Densitometry of the protein levels on Western blots was performed using ImageJ software. Results were analyzed by a paired *t* test or by one-way analysis of variance, followed by Tukey's *post hoc* comparison or by a paired Student's *t* test, using GraphPad Prism (version 5.0) software.

RESULTS

PTCH1-induced apoptosis requires its CTD and is independent of SMO. To determine if the proapoptotic activity of PTCH1 is dependent on SMO or if it constitutes a true form of noncanonical signaling, we tested the function of PTCH1 in $SMO^{-/-}$ MEFs. PTCH1 overexpression in $SMO^{-/-}$ MEFs via adenoviral transduction resulted in significantly increased apoptotic cell death, as determined by a 50 to 70% increase in caspase-3/7 activity (Fig. 1A) and an ~30% reduction in total cell number (Fig. 1B). Deletion of the CTD of PTCH1 resulted in the complete abrogation of its proapoptotic function (Fig. 1A and B). PTCH2, which has a high degree of homology to PTCH1 except in the CTD, was also devoid of proapoptotic activity. Reexpression of SMO in those cells not only did not reduce the apoptotic effect of PTCH1 but also resulted in a higher level of caspase-3/7 activation by PTCH1 (Fig. 1C). Altogether, these data support the notion that PTCH1 induces apoptotic cell death in an SMO-independent manner (type I noncanonical Hh pathway) specifically through the CTD.

The C-terminal tail of PTCH1, but not that of PTCH2, interacts with two Nedd4-family E3 ligases. Our data suggested that the main proapoptotic region was encoded in a part of the PTCH1 CTD (CTD1) not present in the CTD of PTCH2 (CTD2). To investigate protein-protein interactions specific to CTD1 that could shed light on the regulation of the proapoptotic activity of PTCH1, we expressed membrane-bound GFP-CTD1 or GFP-CTD2 fusion proteins in HEK293T cells (Fig. 2A), immunoprecipitated the bait proteins with an anti-GFP antibody, and identified specific interacting proteins by Coomassie blue staining and mass spectrometry. Two protein bands that coprecipitated with CTD1 but not with GFP alone or GFP-CTD2 were further identified by mass spectrometry as the ubiquitin E3 ligases Itch and WWP2 (Fig. 2B). To confirm those interactions, we coexpressed myc-tagged Itch or myc-tagged WWP2 with HA-tagged CTD1 and were able to detect Itch and WWP2 in HA-directed immunoprecipitates (Fig. 2C). The interactions are meaningful since endogenous Itch and WWP2 interact with endogenous PTCH1 in HEK293T cells and in MiaPaca2 pancreatic cancer cells (Fig. 2D). In agreement with these findings, immunofluorescence analysis revealed a significant presence of myc-Itch and myc-WWP2 at loci containing eGFP-PTCH1 (Fig. 2E).

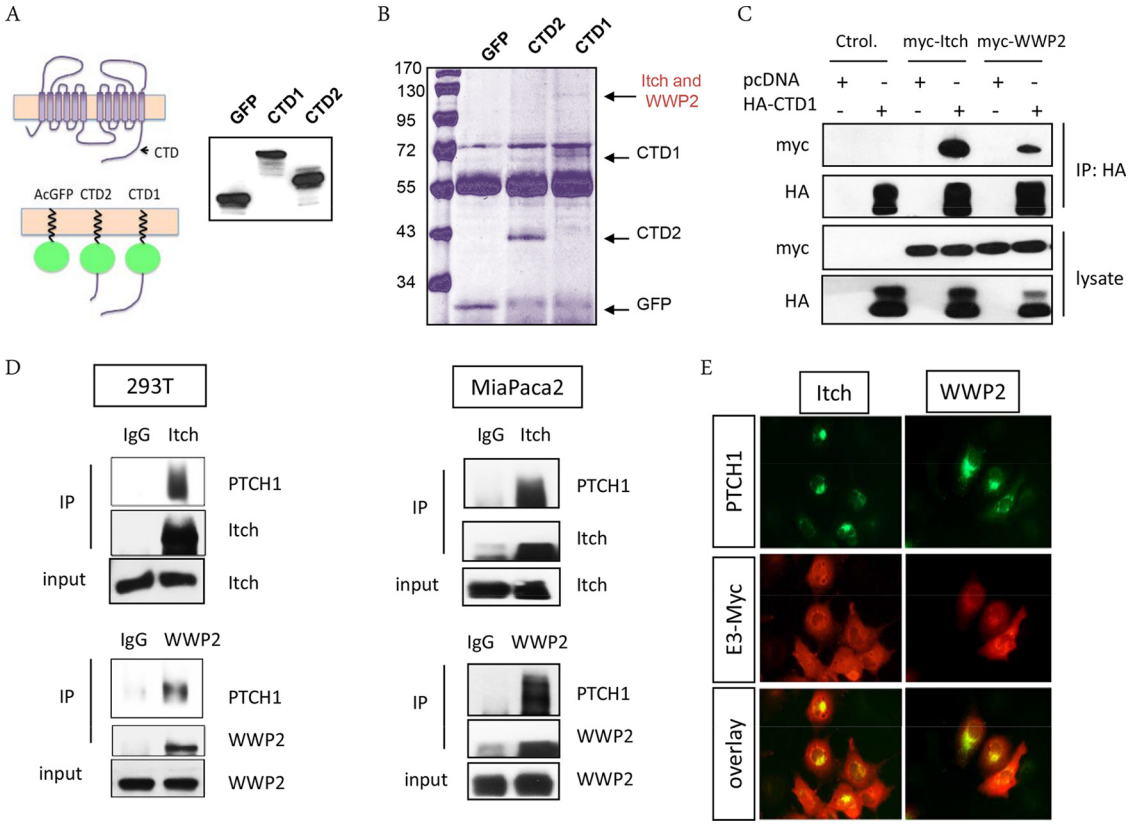

FIG 2 The proapoptotic C-terminal domain of PTCH1 interacts with AIP4 and WWP2. (A) Diagrammatic view and Western blot of the membrane-targeted GFP fusion constructs utilized for pulldown and mass spectrometry. AcGFP, acetylated GFP. (B) Whole-cell lysates of HEK293T cells transfected with a plasmid encoding myr-GFP or fusions of myr-GFP with the C-terminal domain of PTCH1 (CTD1) or PTCH2 (CTD2) were immunoprecipitated under nondenaturing conditions with an anti-eGFP antibody and separated by SDS-PAGE. Coomassie blue staining shows the primary IP products and the co-IP bands used for mass spectrometry. (C) Representative Western blots of samples after co-IP of HA-tagged CTD1 and myc-tagged Itch or WWP2 expressed in HEK293T cells, using a 1:100 dilution of anti-HA antibody (top two gels) and loading controls (lysate; bottom two gels). Ctrol., control. (D) Co-IP of endogenous PTCH1 with endogenous Itch and WWP2 in HEK293T (293T) cells (left) and MiaPaca2 cells (right). Briefly, cell lysates were separated into two aliquots, and one was immunoprecipitated with 2 μg anti-Itch or anti-WWP2 and the other was immunoprecipitated with isotypic IgG as a negative control. The immunoprecipitates were probed for the PTCH1 C53A3 mutant and Itch or WWP2, all at a 1:1,000 dilution. The bottom sets of gels show the levels of the E3 ligases in the starting aliquots. (E) Immunofluorescence of COS-1 cells transfected with vectors encoding PTCH1-HA (green) together with the myc-tagged (E3-myc; red) Itch or WWP2.

Itch displays high selectivity for PTCH1 ubiquitylation among other Nedd4 family members. To determine if other Nedd4-like family E3 ligases also interact with PTCH1 CTD, as recently described for Smurf1 and Smurf2 (26), we coexpressed HA-tagged CTD1 (HA-CTD1) with five additional closely related ligases: Nedd4, Nedd4-2, Smurf1, Smurf2, and WWP1. Immunoprecipitation of HA-CTD1 under nondenaturing conditions coprecipitated all ligases, albeit to different extents (Fig. 3A). Itch and WWP2 showed a strong interaction with CTD1, in agreement with their initial identification by mass spectrometry. However, expression of Itch induced the strongest ubiquitylation of the CTD of PTCH1 in comparison with the level of ubiquitylation obtained with all the other Nedd4 family members, including WWP2 (Fig. 3B). In agreement with this finding, depletion of endogenous Itch in HEK293T cells by two different siRNA duplexes strongly reduced the basal ubiquitylation level of full-length PTCH1 (Fig. 3C), supporting the notion that Itch is the main E3 ubiquitin ligase for PTCH1 in the absence of Hedgehog ligands.

Itch promotes PTCH1 degradation. Because the primary roles of ubiquitylation are protein sorting and degradation, we investigated the effect of Itch and WWP2 on PTCH1 degradation. Overexpression of Itch strongly reduced PTCH1 levels (Fig. 4A), in agreement with the increased ubiquitylation shown in Fig. 3B. The catalytic activity of Itch was essential for PTCH1 degradation, since the catalytically inactive mutant Itch (C830A) did not stimulate PTCH1 degradation (Fig. 4A). In contrast, WWP2 had a minor effect, consistent with the weaker ubiquitylation of PTCH1 shown before. In addition, mutation of the caspase cleavage site of the PTCH1 CTD (D1392N) did not affect PTCH1 degradation by Itch (data not shown). To confirm that Itch is the main regulator of resting PTCH1 levels, we depleted endogenous Itch using two different siRNA duplexes in HEK293T cells stably expressing PTCH1. Reduction of Itch expression resulted in a concomitant increase in steady-state PTCH1 levels of more than 2-fold (Fig. 4B). In contrast, depletion of WWP2 did not affect PTCH1 stability, in agreement with the weaker effect of overexpressed WWP2 on PTCH1 ubiquitylation and degradation (Fig. 4B).

Because all other Nedd4 ligase family members also interact with PTCH1, we tested if they promote its degradation. A comprehensive comparison revealed that in addition to Itch, Smurf2 is the only other E3 ligase that affects the steady-state levels of PTCH1 (Fig. 4C), as recently reported (26). However, the role of

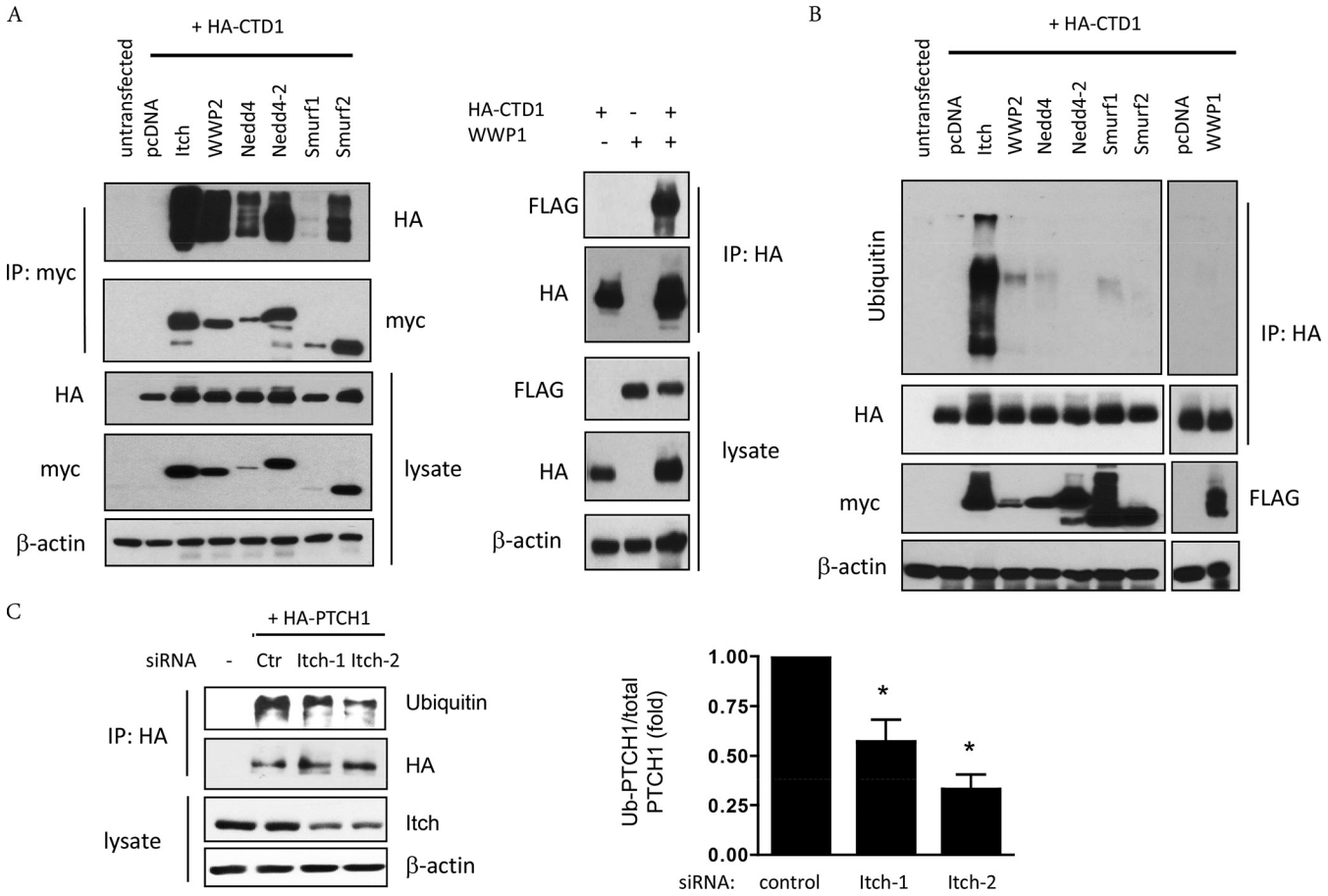

FIG 3 Itch is the preferential E3 ubiquitin-protein ligase for PTCH1 in the absence of Hh proteins. (A) (Left) HEK293T cells were transfected with HA-CTD1 and an equal amount of the indicated myc-tagged Nedd4-family E3 ligases. After 18 h, cell lysates were immunoprecipitated with an anti-myc monoclonal antibody (9B11; 1:100 dilution) to immunoprecipitate all ligases except WWP1, and the IP products were probed for HA and myc. (Right) Cells were transfected with HA-CTD1 and FLAG-WWP1, immunoprecipitated with anti-HA antibody (1:100 dilution; Pierce), and blotted against HA and FLAG. (B) HEK293T cells were transfected with HA-CTD1 and the indicated myc-tagged or FLAG-tagged Nedd4-family E3 ligases. After 18 h, MG132 was added at 10 μM to prevent the degradation of ubiquitylated proteins. At 24 h posttransfection, HA-CTD1 was immunoprecipitated under denaturing conditions in the presence of 10 mM NEN and the immunoprecipitates were blotted for HA and ubiquitin. (C) HEK293T cells were transfected with 5 nM control (Ctr) siRNA or siRNA duplexes targeting Itch using HiPerFect transfection reagent. After 2 days, they were transfected with HA-PTCH1 using Lipofectamine 2000 and treated with MG132 for 18 h. PTCH1 was immunoprecipitated with the HA antibody as described for panel B and probed for ubiquitin. The bar graph represents the ratio of ubiquitylated PTCH1 over total PTCH1, obtained by densitometry, in cells treated with control or Itch-directed siRNA ($n = 3$; *, $P < 0.01$).

Itch in the regulation of PTCH1 levels has a deep biological significance, as overexpression of Itch in NIH 3T3 cells was sufficient to induce spontaneous Gli luciferase activity (Fig. 4D), suggesting that the loss of endogenous PTCH1 by Itch-mediated ubiquitylation and degradation is enough to derepress SMO and initiate canonical Hh signaling in the absence of an Hh ligand. Altogether, these results suggest that Itch regulates PTCH1 recycling in the absence of Hh ligand via interaction with the CTD and the transfer of ubiquitin to PTCH1.

The interaction of Itch and WWP2 with PTCH1 is dependent on two PPXY motifs. Itch and WWP2 contain four WW domains that serve for substrate recognition through binding to a PY motif, usually PPXY (27). PTCH1 contains one PPPY stretch in the CTD that is the candidate site for E3 ligase recognition. As shown in Fig. 5, mutation of the C-terminal PPPY motif to PPPA (C-PPPA) strongly reduced the physical association of Itch and WWP2 with PTCH1 but did not abolish it. PTCH1 also contains in its large intracellular loop another cytoplasmic PPXY motif which is not conserved in PTCH2. Mutation of the loop PPXY motif (L-PPPA) did not significantly affect the association with Itch or WWP2, but mutation of both the C-terminal and loop PPXY motifs (LC-PPPA) completely abrogated the interaction of PTCH1 with both E3 ligases (Fig. 5).

Itch mediates PTCH1 ubiquitylation at K1413. The CTD of PTCH1 contains a single candidate ubiquitylation site (K1413 in human PTCH1) that is absent in PTCH2, and we hypothesized that this is the main target site of Itch. We first established if K1413 is ubiquitylated *in vivo*. Wild-type HA-tagged CTD1 is ubiquitylated when expressed in HEK293T cells, while a K1413R mutant CTD1 is not (Fig. 6A). Moreover, coexpression of wild-type CTD1 with Itch leads to a dramatic increase in ubiquitylation in comparison to the endogenous level; ubiquitylation is abolished in the K1413R mutant (Fig. 6B). We believe that the high-molecular-weight ubiquitin signal that is immunoprecipitated with both wild-type and K1413R mutant HA-CTD1 likely represents the autoubiquitylation of the Itch that is coimmunoprecipitated with

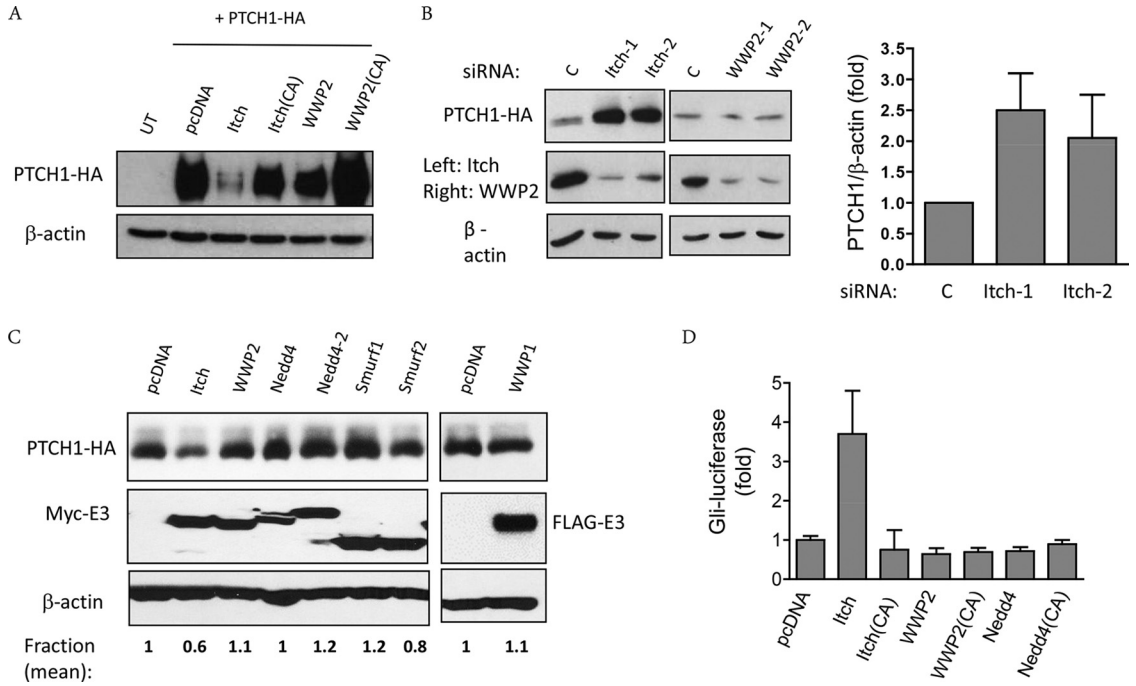

FIG 4 Itch controls PTCH1 degradation in the absence of Hh ligands. (A) Level of PTCH1 expression in HEK293T cells transfected with HA-PTCH1 and empty vector (pcDNA; UT, untransfected), wild-type Itch (Itch), catalytically inactive Itch [Itch(CA)], wild-type WWP2 (WWP2), or catalytically inactive WWP2 [WWP2(CA)]. (B) HEK293T cells stably transfected with doxycycline-inducible HA-PTCH1 express very small leaky amounts of HA-PTCH1 that are comparable to the levels of endogenous protein expression. Depletion of Itch with two different siRNA duplexes at 5 nM with HiPerFect transfection reagent for 72 h resulted in a strong increase in leaky HA-PTCH1 levels, but depletion of WWP2 did not. The bar graph below the gels shows the quantitative data from 3 independent experiments. C, control. (C) HEK293T cells stably transfected with doxycycline-inducible HA-PTCH1 were transiently transfected with PTCH1-HA and the indicated E3 ligases belonging to the Nedd4 family (all tagged with myc, except WWP1, which was tagged with FLAG). Cell lysates were immunoblotted to determine the levels of PTCH1-HA and the expression of the E3 ligases. The fraction of PTCH1-HA normalized to the amount of the empty vector was quantified by densitometry (results are the means of 3 independent experiments). (D) Normalized Gli luciferase reporter activity in NIH 3T3 cells at 18 h after transfection with the empty vector (pcDNA) or with myc-tagged Itch, catalytically inactive Itch, WWP2, catalytically inactive WWP2, Nedd4, and catalytically inactive Nedd4 [Nedd4(CA)] using the Fugene HD reagent. The results on the graph represents the means ± SEMs of 3 independent experiments ($P < 0.05$, Itch vs. all other groups).

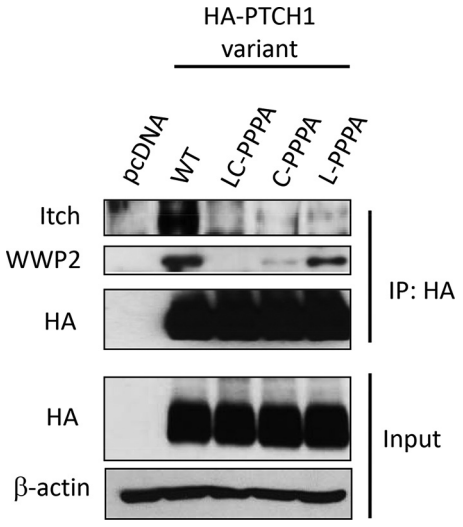

FIG 5 Itch and WWP2 interact with PTCH1 through two PPXY motifs. HEK293T cells were transfected for 18 h with wild-type (WT) PTCH1-HA, PTCH1-HA mutated in the C-terminal domain PPXY motif (C-PPXA), PTCH1-HA mutated in the central loop PPXY motif (L-PPXA), or a PTCH1-HA variant mutated in the two PPXY motifs (LC-PPXA). Immunoprecipitates of each HA-PTCH1 variant were probed for associated endogenous Itch and WWP2 by Western blotting.

the CTD (28). In agreement with the findings presented above, mutation of K1413 strongly reduced CTD1 and full-length PTCH1 degradation under resting conditions (Fig. 6C and D). It is possible that the remaining degradation of PTCH1 K1413R is mediated via cointernalization with endogenous wild-type PTCH1. It was previously reported that *Drosophila melanogaster* Patched (Ptc) forms dimers or trimers (29). In our study, we were able to demonstrate that the isolated human CTD1 interacts with full-length PTCH1 both by coimmunoprecipitation and by colocalization when PTCH1 is coexpressed, with staining changing from diffuse cytoplasmic and nuclear staining to punctate cytoplasmic and membrane staining (data not shown). Thus, it is possible that ubiquitylation of endogenous PTCH1 mediates the internalization and degradation of the physically associated PTCH1 K1413R mutant. Moreover, while PTCH1 has 14 additional Lys residues in intracytoplasmic loops besides K1413, the mutation of K1413 alone strongly reduced the ability of Itch to induce PTCH1 degradation (Fig. 6E). The PTCH1 K1413R mutant was more stable and more resistant to degradation by both proteasomal and lysosomal pathways, as shown by the differential effects of proteasomal inhibitors (MG132 and lactacystin) and a lysosomal inhibitor (ammonium chloride) (Fig. 6F). These data underscore the importance of K1413 in the regulation of the basal turnover of PTCH1.

Ubiquitylation promotes PTCH1 endocytosis. Although

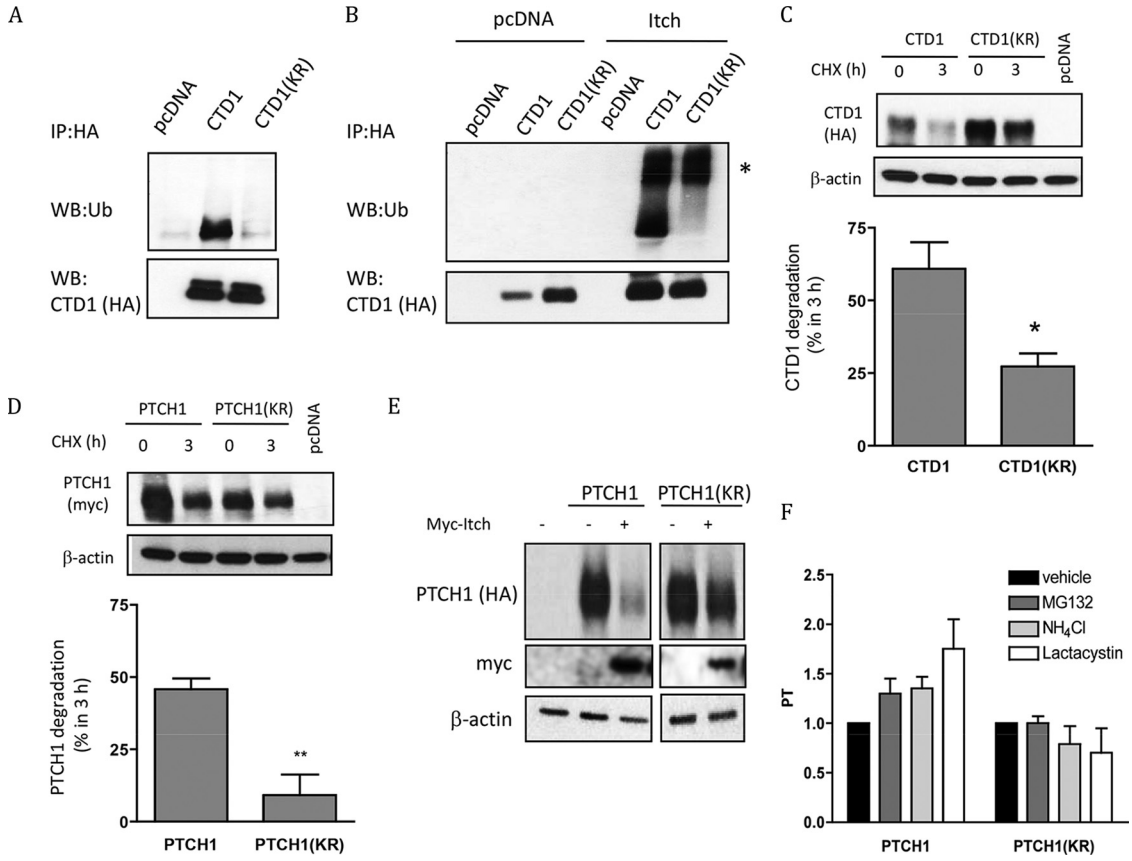

FIG 6 PTCH1 is ubiquitylated by Itch on K1413. (A) Expression of HA-tagged CTD1 or a CTD1 K1413R mutant [CTD1(KR)] in HEK293T cells, followed by lysis under denaturing conditions, immunoprecipitation with an anti-HA antibody, and immunoblotting for ubiquitin. WB, Western blotting. (B) Cells transfected as described in the legend to panel A with or without myc-Itch were incubated with cycloheximide (CHX) for 3 h and lysed, and the levels of ubiquitylation of CTD1 were evaluated by Western blotting. *, the upper band might represent autoubiquitylation of Itch, which immunoprecipitates with HA-CTD1. (C) Densitometric quantification of CTD1 and CTD1(KR) degradation, normalized to the level of β-actin expression, expressed as the percent reduction after 3 h ($n = 3$; *, $P < 0.05$). (D) Same as panel C but using full-length HA-PTCH1 and the full-length HA-tagged PTCH1 K1413R mutant ($n = 3$; **, $P < 0.01$). (E) Stability of full-length HA-PTCH1 and the PTCH1 K1413 mutant when cotransfected with empty vector (pcDNA) or myc-Itch in HEK293T cells. (F) Densitometric quantification of HA-PTCH1 and HA-tagged PTCH1 K1413R mutant levels in HEK293T cells treated with vehicle or the proteasome for 3 h ($n = 3$).

PTCH1 is a membrane receptor for the Hh ligands, at steady state the largest fraction of PTCH1 is found in intracellular structures, including vesicles and the perinuclear region, consistent with its expected biosynthetic transport through the Golgi apparatus and trans-Golgi network (Fig. 2E and 7A and B). A weak signal at the plasma membrane could be detected after overexposure and mostly at early times posttransfection (Fig. 7A), suggesting that PTCH1 is actively internalized. Double immunostaining revealed substantial colocalization with ubiquitin, especially in the intracellular vesicles (Fig. 7A), supporting the notion that ubiquitylation might promote the endocytosis of PTCH1. Indeed, mutation of K1413 led to an increase in full-length PTCH1 and CTD1 plasma membrane localization, suggesting that ubiquitylation at K1413 promotes internalization (Fig. 7B). To confirm this observation, we used intact cell surface protein biotinylation to label the fraction of PTCH1 exposed to the extracellular milieu during a brief time window of 30 min. We compared the membrane levels of the PTCH1 D1392N mutant, a mutant with a mutation in the caspase cleavage site unable to trigger apoptosis, with those of the PTCH1 D1392N and K1413R double mutant. As shown in Fig. 7C, quantitation revealed a significant accumulation of the PTCH1 D1392N and K1413R mutant at the plasma membrane compared to level of accumulation for the single mutant, supporting the notion that ubiquitylation of the CTD, in addition to functioning in PTCH1 degradation, stimulates PTCH1 endocytosis and that defective ubiquitylation compromises internalization. The role of ubiquitylation in PTCH1 internalization is also supported by the striking change in subcellular localization of PTCH1 when coexpressed with Itch. As shown in Fig. 7D, Itch induced a strong perinuclear aggregation of PTCH1, while the catalytically dead Itch C380A mutant did not. The number of cells with disperse vesicular staining of PTCH1 was reduced at the expense of cells showing a single perinuclear aggregate that resembles the aggresome (Fig. 7D).

Shh stimulates degradation of PTCH1 through increased ubiquitylation. We next sought to investigate if Shh affects the turnover of mammalian PTCH1. Addition of recombinant Shh to cells expressing PTCH1-HA under the control of the cytomegalovirus (CMV) promoter resulted in the degradation of ectopic PTCH1 in a dose- and time-dependent manner (Fig. 8A and B). Addition of Shh also increased overall PTCH1 ubiquitylation and promoted an additional molecular weight shift, which was abol-

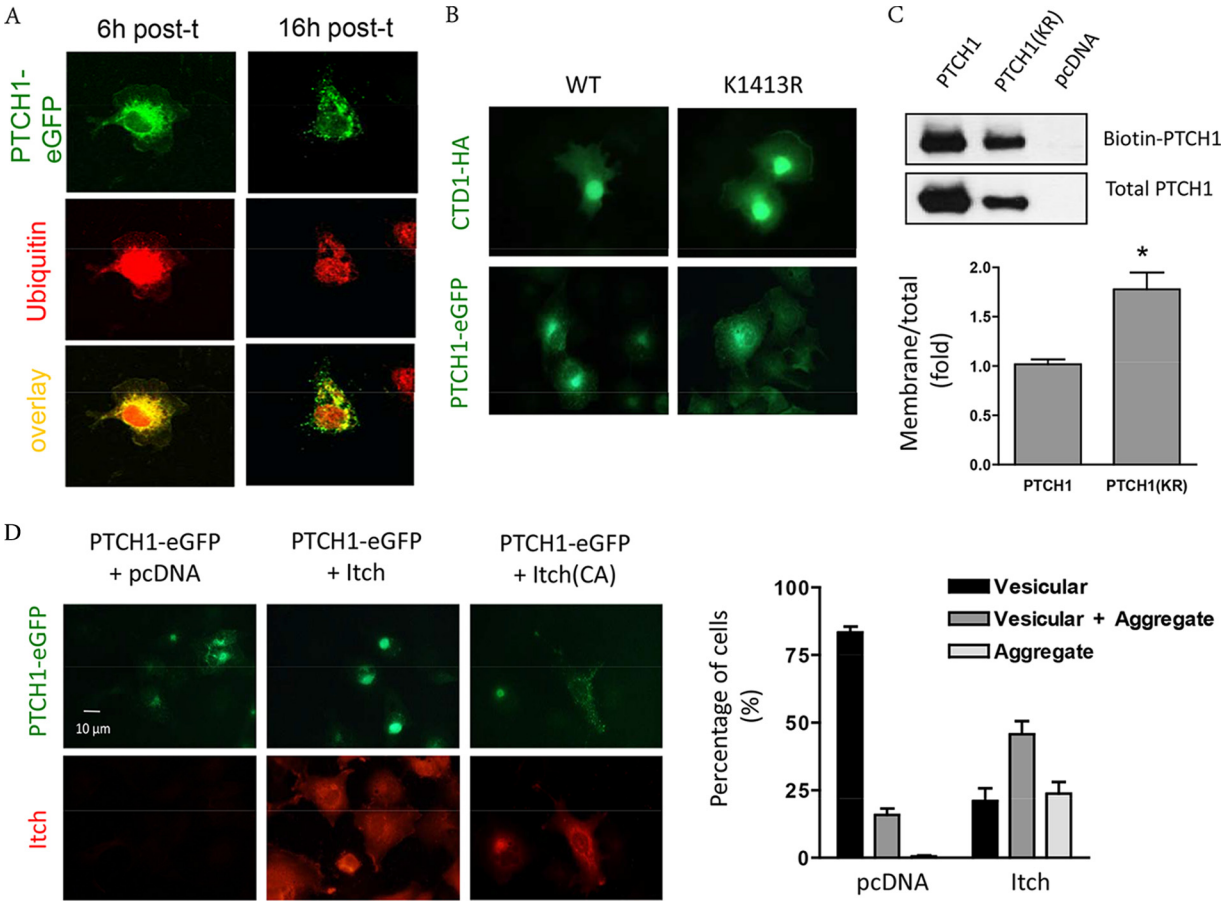

FIG 7 Regulation of PTCH1 plasma membrane retention by K1413. (A) Colocalization of PTCH1-eGFP (green) and endogenous ubiquitin (red) in COS-1 cells at 6 h and 16 h posttransfection (post-t). (B) Subcellular localization of wild-type PTCH1-eGFP and HA-CTD1 and their K1413R mutants (green) shows increased plasma membrane levels of the K1413R mutants. (C) HEK293T cells expressing empty vector (pcDNA), PTCH1-HA, or the PTCH1 K1413R variant [PTCH1(KR)] were biotinylated as indicated in Materials and Methods. PTCH1-HA pulled down with avidin-labeled beads and total lysate PTCH1-HA were quantified by densitometry (right) after immunoblotting with an anti-HA antibody (left) ($n = 3$; *, $P < 0.01$). (D) (Left) Subcellular distribution of PTCH1-eGFP coexpressed in HEK293T cells with empty plasmid (pcDNA), myc-Itch, or catalytically inactive myc-Itch. (Right) Percentage of cells showing punctate staining (vesicular), perinuclear aggregates, or a mixed of the two. Values are means ± SEMs of 3 experiments.

ished by mutation of K1413 (Fig. 8C). It is noteworthy that while K1413 is a critical determinant for PTCH1 degradation, the ubiquitylation of other sites is still substantial in the PTCH1 K1413R mutant. Despite the role of K1413 in Shh-induced PTCH1 degradation, depletion of Itch did not prevent the degradation of PTCH1 by Shh (Fig. 8D). Therefore, it seems that Itch regulates basal PTCH1 turnover in the absence of ligand, while a different E3 ligase takes over the control of PTCH1 regulation in the presence of Shh.

Ubiquitylation of K1413 modulates the proapoptotic activity of PTCH1 in the absence of Sonic Hedgehog. Because the PTCH1 K1413R mutant has increased stability, we expected it to be more active than wild-type PTCH1 in its inhibition of canonical Hh signaling and promotion of noncanonical Hh signaling. To study its ability to repress SMO and prevent Gli activation, hallmarks of the canonical Hh pathway, we used $Ptc1^{-/-}$ MEFs, in which constitutive activation of the canonical Hh pathway by a lack of endogenous Ptc1 results in high levels of Gli-dependent transcription in the absence of ligand (30). The potencies of inhibition of Gli transcriptional activity by PTCH1 and the PTCH1 K1413R mutant transfected into Ptc1-deficient MEFs were similar and were comparable to the potency of the SMO inhibitor KAAD-cyclopamine, and PTCH1 and the PTCH1 K1413R mutant were similarly regulated by Shh, as determined using a Gli luciferase reporter (data not shown). In agreement with those findings, both PTCH1 and the PTCH1 K1413R mutant could be detected at the primary cilium in $Ptc1^{-/-}$ MEFs, an event necessary for inhibition of SMO- and Gli-dependent transcription (data not shown).

In contrast to the lack of an effect of K1413 ubiquitylation on the regulation of the canonical Hh pathway, the PTCH1 K1413R mutant was 2.2-fold more active in the induction of cell death than wild-type PTCH1 in HEK293T cells (Fig. 9A). Importantly, the proapoptotic activity was still regulated by Shh. The reason for this is unknown, but we speculate that the K1413R mutant might be coregulated with endogenous wild-type PTCH1 via homotypic interactions. Immunoprecipitation of PTCH1 and the PTCH1 K1413R mutant revealed that the ubiquitylation-deficient mutant had an increased affinity for caspase-9 (Fig. 9B) but a decreased affinity for DRAL (Fig. 9C), indicating that the ubiquitylation of K1413 remodels the proapoptotic complex, or dependosome, activated by PTCH1. Remarkably, the activity of caspase-9 associated with PTCH1 was dramatically increased by the K1413R mu-

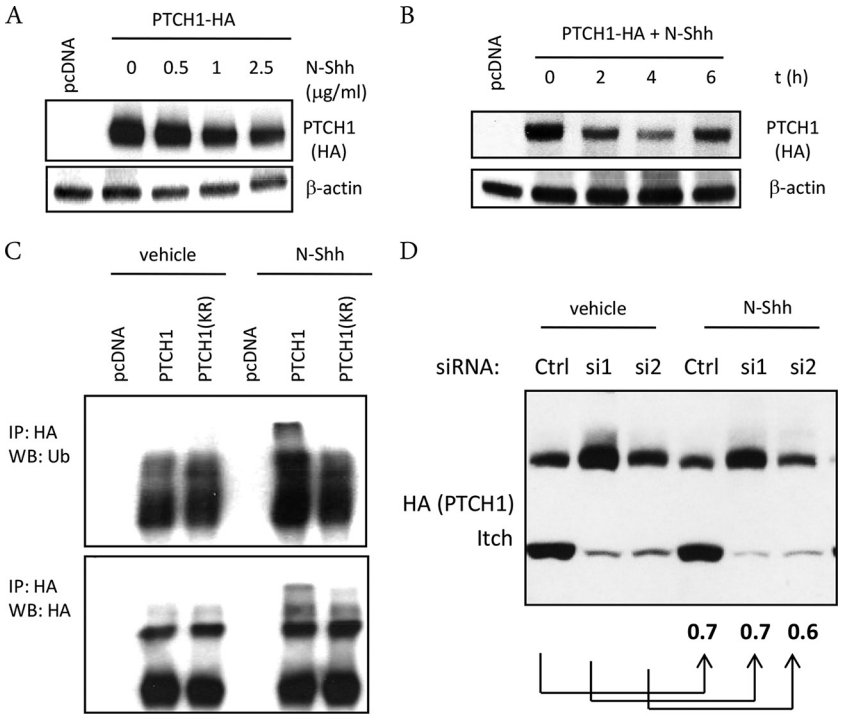

FIG 8 Sonic Hedgehog promotes ubiquitylation at K1413 and degradation of PTCH1. (A) PTCH1-HA expression levels in HEK293T cells after 4 h of stimulation with increasing concentrations of the N-terminal fragment of Shh (N-Shh), from 0 to 2.5 μg/ml. (B) Time-dependent degradation of PTCH1-HA in HEK293T cells incubated with 2.5 μg/ml Shh for the indicated times (t). (C) Cells transfected with empty vector (pcDNA), PTCH1-HA, or PTCH1(KR)-HA were treated simultaneously with 20 μM MG132 and 2.5 μg/ml Shh, lysed after 4 h under denaturing conditions, and immunoprecipitated with an anti-HA antibody, followed by immunoblotting against ubiquitin (top) and HA (bottom). (D) HEK293T cells transfected with 5 nM control (Ctrl) or two different Itch siRNAs (si1 and si2) for 72 h were transfected with HA-PTCH1 and at 18 h posttransfection were stimulated with 2.5 μg/ml Shh for 4 h. The levels of PTCH1-HA and Itch were determined by Western blotting. The fraction of PTCH1 remaining at 4 h is indicated by the numbers under the gel.

tation (Fig. 9D), providing a mechanism for the net increase in cell death. Altogether, our findings indicate that K1413 ubiquitylation exclusively reduces the apoptotic potential of PTCH1 (noncanonical Hh signaling type I) by modifying the apoptotic complex stoichiometry and caspase-9 activation without apparently affecting canonical Hh signaling.

DISCUSSION

In this study, we demonstrate for the first time that resting plasma membrane levels of PTCH1 are regulated by the ubiquitylation of K1413 in the C-terminal domain mediated by the Nedd4 family member Itch. Our data indicate that ubiquitylation promotes internalization and proteasomal degradation of PTCH1, which are essential to limit the proapoptotic activity of unliganded PTCH1, a form of type II noncanonical Hh signaling. Remarkably, PTCH1 ubiquitylation at K1413 is not required for Shh-mediated inhibition and degradation of PTCH1 and thus is dispensable for activation of canonical Hh signaling. Incidentally, a recent report points to Smurf proteins as being the E3 ligases that regulate Shh-dependent PTCH1 turnover and that have a more influential role on canonical Hh signaling (26). It is remarkable that two Nedd4 family members appear to play differential roles in PTCH1 ubiquitylation. Our study shows that Itch is the Nedd4 family member that is the most active toward PTCH1 in the absence of Hh ligands. We tested and confirmed that while PTCH1 interacts with most Nedd4 family members (Nedd4, Nedd4-2, WWP1, WWP2, Itch, Smurf1, and Smurf2), unliganded PTCH1 is a preferred substrate for Itch. To our knowledge, this is the first report of a biased utilization of different E3 ligases for PTCH1 regulation in canonical versus noncanonical Hh signal transduction.

The Nedd4 family of E3 ligases has also been linked to other aspects of Hh signaling. Itch was found to mediate Gli1 turnover by ubiquitylation in the presence of the adaptor protein Numb (31). Thus, the two most upregulated proteins by the canonical Hh signaling, PTCH1 and Gli1, are substrates of Itch. In addition, binding of Nedd4 to PTCH1 facilitates ubiquitylation of a PTCH1-interacting protein of the dependosome complex, caspase-9, which results in its activation (32). Therefore, the expression levels of different Nedd4 family members and their regulators may contribute to the intrinsic cell type-specific strength of Hh signaling.

Our findings suggest that K1413 ubiquitylation is not essential for inhibition of PTCH1 canonical and noncanonical functions by Shh. First, the K1413R mutant accumulates at the cilium membrane under resting conditions, and addition of Shh derepresses Gli transcriptional activation. Canonical Hh signaling requires endocytosis of PTCH1 from the primary cilium membrane (33–35). Many ciliary proteins are endocytosed via a clathrin-coated ciliary pocket structure located at the base of the cilium (36). If this is the case for PTCH1, trafficking to and from the cilium does not require K1413 ubiquitylation.

However, in the absence of Hh ligands, the K1413R mutant is present at a higher level than wild-type PTCH1 at the plasma membrane and has a slower turnover. In a complementary exper-

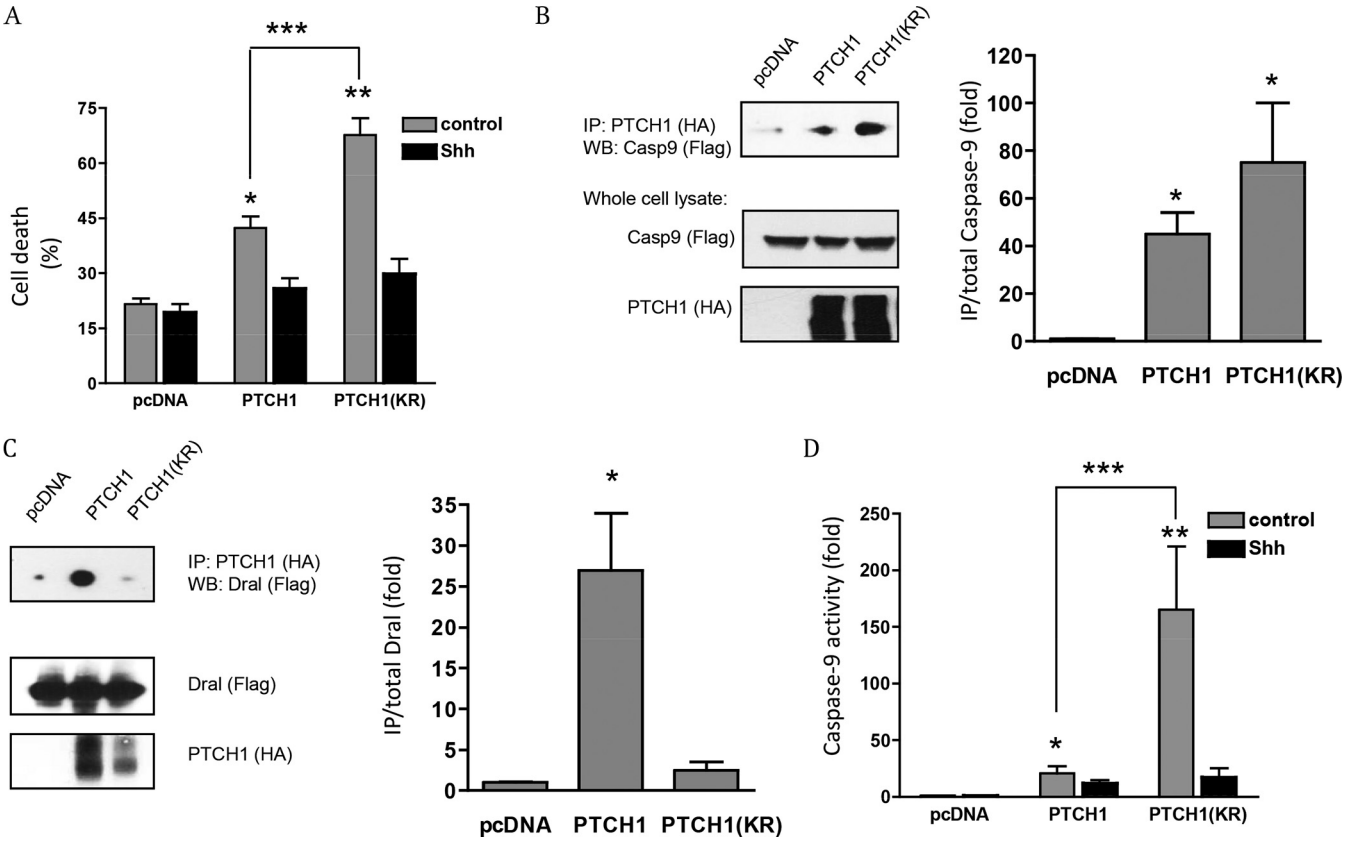

FIG 9 K1413 selectively regulates cell death induced by PTCH1 overexpression. (A) Cell death, as a percentage of the number of trypan blue-positive cells, in HEK293T cells transfected with pcDNA, PTCH1-HA, or PTCH1(KR)-HA and incubated or not with Shh for 48 h ($n = 9$; *, $P < 0.0001$; **, $P < 0.001$; ***, $P < 0.05$). (B) Coimmunoprecipitation of caspase-9 (Casp9) with PTCH1-HA or the PTCH1 K1413R mutant using an anti-PTCH1 antibody, followed by Western blotting with an anti-caspase-9 antibody. (Left) Representative Western blot; (right) densitometric quantification of relative caspase-9 coimmunoprecipitation ($n = 3$; *, $P < 0.05$). (C) Coimmunoprecipitation of DRAL with PTCH1-HA or the K1413R mutant, as described in the legend to panel B. (Left) Representative Western blot; (right) densitometric quantification of relative DRAL coimmunoprecipitation ($n = 3$; *, $P < 0.05$). (D) Determination of caspase-9 activity associated with PTCH1 in immunoprecipitates of cells transfected with empty vector (pcDNA), PTCH1-HA, or PTCH1(KR)-HA and stimulated with or without Shh ($n = 4$; *, $P < 0.001$ versus control; **, $P < 0.05$ versus control; ***, $P < 0.05$ for wild type versus KR mutant).

iment, overexpression of Itch sufficed to induce a Gli luciferase reporter in the absence of Shh and to promote the internalization and aggregation of PTCH1. Our study suggests that internalization of the plasma membrane pool of PTCH1 is stimulated by K1413 ubiquitylation by Itch and, to a lesser degree, by WWP2.

Upon ubiquitylation, PTCH1 is degraded by both proteasome and lysosome pathways. Mono- and polyubiquitylation have been reported to promote receptor degradation through both pathways, such as in the case of SMO (37, 38). PTCH1 degradation by lysosomes could result from autophagy of endoplasmic reticulum-derived membranes containing PTCH1 when they fuse with lysosomes to form the autophagosome. The latter is supported by evidence that shows that PTCH1 regulates autophagy (39; X. L. Chen and N. A. Riobo, unpublished observations). Considering the importance of PTCH1 in tissue homeostasis and embryonic development, it is conceivable that there is more than one mechanism to control its protein level. This is extremely important for any dependence receptor to avoid triggering massive apoptosis in the absence of ligand.

Drosophila Patched (Ptc), which has a CTD highly homologous to that of PTCH1, was reported by different investigators to associate with Nedd4 and Smurf through a PPXY motif (29, 40). In the fruit fly, the Nedd4 family is composed of three members: Nedd4, Smurf, and Suppressor of deltex (41). Smurf was shown to induce Ptc ubiquitylation and degradation in cultured S2 cells and in the wing disc, while Nedd4 was also shown to reduce the half-life of Ptc (29, 40). Interaction with both E3 ligases depends on the CTD PPXY motif, and mutation to PPXA results in the aberrant internalization of Ptc and inhibition of Hh-stimulated transcriptional activity of cubitus interruptus (Ci) (29, 40). The importance of the CTD of Ptc/PTCH1 in the regulation of its stability and turnover is thus conserved across phyla. However, in vertebrates ubiquitylation of the CTD is also finely regulated in the absence of ligand, given its function as a dependence receptor, and it seems that the use of different E3 ligases has been refined for the individual conformations of PTCH1. Moreover, mammalian PTCH1 serves as a docking site for Nedd4 to act on caspase-9, promoting its activation and apoptosis (32). It makes sense, therefore, that Nedd4 does not target PTCH1 significantly because that will result in the opposite, attenuation of cell death. Thus, ubiquitylation plays a central regulatory role in the proapoptotic function of PTCH1 by modification of both PTCH1 and its associated proteins.

In mouse models of Itch deficiency, mice develop a severe au-

toimmune disease and are characterized by intense scratching (itchy phenotype) but do not show any gross patterning defects related to canonical Hh signaling (42). This could be the result of redundancy with other Nedd4 family members and/or to the fact that Itch targets multiple substrates in the Hh signaling network and other developmental pathways, such as Notch (31, 42). However, homozygous mutations in Itch in humans were associated with a hereditary multisystem autoimmune disease that also encompasses organomegaly and craniofacial abnormalities, which could be related to the dysregulation of PTCH1 (42).

An inhibitory role of K1413 in PTCH1-induced cell death is consistent with the finding that the proapoptotic activity requires cleavage of PTCH1 at D1392, which results in removal of the single ubiquitylation site (11). We predict that after K1413 is eliminated, the cleaved PTCH1 has higher membrane stability and at the same time allows ubiquitylation of caspase-9 by Nedd4, since the remaining portion of the CTD retains the PPXY motif. Here we show that abrogation of CTD PTCH1 ubiquitylation in the intact molecule also enhances caspase-9 activity. Together, these observations suggest that the apoptotic potential of PTCH1 is regulated by K1413 ubiquitylation by Itch. In summary, it is probable that K1413 ubiquitylation opposes PTCH1-initiated cell death by two mechanisms: increased internalization/degradation and remodeling of the proapoptotic complex.

Altogether, our data support a model of selective modulation of PTCH1 activity in type I noncanonical Hh signaling by ubiquitylation of K1413 by Itch, which reorganizes the proapoptotic complex and is followed by internalization and degradation. This is the first report of a single-site modification of PTCH1 that exclusively regulates its noncanonical function but does not affect Gli-dependent transcription.

ACKNOWLEDGMENTS

National Institutes of Health grant RO1-GM88526 to N.A.R. and the W. W. Smith Charitable Foundation funded this work.

P.M. declares a conflict of interest as a founder of and shareholder in Netris Pharma.

REFERENCES

1. **Carpenter D, Stone DM, Brush J, Ryan A, Armanini M, Frantz G, Rosenthal A, de Sauvage FJ.** 1998. Characterization of two patched receptors for the vertebrate Hedgehog protein family. Proc. Natl. Acad. Sci. U. S. A. **95:**13630–13634. http://dx.doi.org/10.1073/pnas.95.23.13630.
2. **Robbins DJ, Fei DL, Riobo NA.** 2012. The Hedgehog signal transduction network. Sci. Signal. **5:**re6. http://dx.doi.org/10.1126/scisignal.2002906.
3. **Yang C, Chen W, Chen Y, Jiang J.** 2012. Smoothened transduces Hedgehog signal by forming a complex with Evc/Evc2. Cell Res. **22:**1593–1604. http://dx.doi.org/10.1038/cr.2012.134.
4. **Gailani MR, Stahle-Backdahl M, Leffell DJ, Glynn M, Zaphiropoulos PG, Pressman C, Undén AB, Dean M, Brash DE, Bale AE, Toftgård R.** 1996. The role of the human homologue of Drosophila patched in sporadic basal cell carcinomas. Nat. Genet. **14:**78–81. http://dx.doi.org/10.1038/ng0996-78.
5. **Hahn H, Christiansen J, Wicking C, Zaphiropoulos PG, Chidambaram A, Gerrard B, Vorechovsky I, Bale AE, Toftgard R, Dean M, Wainwright B.** 1996. A mammalian Patched homolog is expressed in target tissues of Sonic Hedgehog and maps to a region associated with developmental abnormalities. J. Biol. Chem. **271:**12125–12128. http://dx.doi.org/10.1074/jbc.271.21.12125.
6. **Johnson RL, Rothman AL, Xie J, Goodrich LV, Bare JW, Bonifas JM, Quinn AG, Myers RM, Cox DR, Epstein EH, Jr, Scott MP.** 1996. Human homolog of Patched, a candidate gene for the basal cell nevus syndrome. Science **272:**1668–1671. http://dx.doi.org/10.1126/science.272.5268.1668.
7. **Xie J, Johnson RL, Zhang X, Bare JW, Waldman FM, Cogen PH, Menon AG, Warren RS, Chen LC, Scott MP, Epstein EH, Jr.** 1997. Mutations of the Patched gene in several types of sporadic extracutaneous tumors. Cancer Res. **57:**2369–2372.
8. **Goodrich LV, Milenkovic L, Higgins KM, Scott MP.** 1997. Altered neural cell fates and medulloblastoma in mouse patched mutants. Science **277:**1109–1113. http://dx.doi.org/10.1126/science.277.5329.1109.
9. **Belyea B, Kephart JG, Blum J, Kirsch DG, Linardic CM.** 2012. Embryonic signaling pathways and rhabdomyosarcoma: contributions to cancer development and opportunities for therapeutic targeting. Sarcoma **2012:**406239. http://dx.doi.org/10.1155/2012/406239.
10. **Lee Y, Miller HL, Russell HR, Boyd K, Curran T, McKinnon PJ.** 2006. Patched2 modulates tumorigenesis in Patched1 heterozygous mice. Cancer Res. **66:**6964–6971. http://dx.doi.org/10.1158/0008-5472.CAN-06-0505.
11. **Thibert C, Teillet MA, Lapointe F, Mazelin L, Le Douarin NM, Mehlen P.** 2003. Inhibition of neuroepithelial Patched-induced apoptosis by Sonic Hedgehog. Science **301:**843–846. http://dx.doi.org/10.1126/science.1085405.
12. **Mille F, Thibert C, Fombonne J, Rama N, Guix C, Hayashi H, Corset V, Reed JC, Mehlen P.** 2009. The Patched dependence receptor triggers apoptosis through a DRAL-caspase-9 complex. Nat. Cell Biol. **11:**739–746. http://dx.doi.org/10.1038/ncb1880.
13. **Mehlen P.** 2003. Patched is a dependence receptor. Med. Sci. (Paris) **19:**1062. http://dx.doi.org/10.1051/medsci/200319111062.
14. **Chinchilla P, Xiao L, Kazanietz MG, Riobo NA.** 2010. Hedgehog proteins activate pro-angiogenic responses in endothelial cells through noncanonical signaling pathways. Cell Cycle **9:**570–579. http://dx.doi.org/10.4161/cc.9.3.10591.
15. **Brennan D, Chen X, Cheng L, Mahoney M, Riobo NA.** 2012. Noncanonical Hedgehog signaling. Vitam. Horm. **88:**55–72. http://dx.doi.org/10.1016/B978-0-12-394622-5.00003-1.
16. **Nieuwenhuis E, Barnfield PC, Makino S, Hui CC.** 2007. Epidermal hyperplasia and expansion of the interfollicular stem cell compartment in mutant mice with a C-terminal truncation of Patched1. Dev. Biol. **308:**547–560. http://dx.doi.org/10.1016/j.ydbio.2007.06.016.
17. **Makino S, Masuya H, Ishijima J, Yada Y, Shiroishi T.** 2001. A spontaneous mouse mutation, mesenchymal dysplasia (mes), is caused by a deletion of the most C-terminal cytoplasmic domain of Patched (Ptc). Dev. Biol. **239:**95–106. http://dx.doi.org/10.1006/dbio.2001.0419.
18. **Acconcia F, Sigismund S, Polo S.** 2009. Ubiquitin in trafficking: the network at work. Exp. Cell Res. **315:**1610–1618. http://dx.doi.org/10.1016/j.yexcr.2008.10.014.
19. **Metzger MB, Hristova VA, Weissman AM.** 2012. HECT and RING finger families of E3 ubiquitin ligases at a glance. J. Cell Sci. **125:**531–537. http://dx.doi.org/10.1242/jcs.091777.
20. **Rotin D, Kumar S.** 2009. Physiological functions of the HECT family of ubiquitin ligases. Nat. Rev. Mol. Cell Biol. **10:**398–409. http://dx.doi.org/10.1038/nrm2690.
21. **Bernassola F, Karin M, Ciechanover A, Melino G.** 2008. The HECT family of E3 ubiquitin ligases: multiple players in cancer development. Cancer Cell **14:**10–21. http://dx.doi.org/10.1016/j.ccr.2008.06.001.
22. **Maddika S, Kavela S, Rani N, Palicharla VR, Pokorny JL, Sarkaria JN, Chen J.** 2011. WWP2 is an E3 ubiquitin ligase for PTEN. Nat. Cell Biol. **13:**728–733. http://dx.doi.org/10.1038/ncb2240.
23. **Chen C, Matesic LE.** 2007. The Nedd4-like family of E3 ubiquitin ligases and cancer. Cancer Metastasis Rev. **26:**587–604. http://dx.doi.org/10.1007/s10555-007-9091-x.
24. **Marchese A, Raiborg C, Santini F, Keen JH, Stenmark H, Benovic JL.** 2003. The E3 ubiquitin ligase AIP4 mediates ubiquitination and sorting of the G protein-coupled receptor CXCR4. Dev. Cell **5:**709–722. http://dx.doi.org/10.1016/S1534-5807(03)00321-6.
25. **Martinez-Chinchilla P, Riobo NA.** 2008. Purification and bioassay of Hedgehog ligands for the study of cell death and survival. Methods Enzymol. **446:**189–204. http://dx.doi.org/10.1016/S0076-6879(08)01611-X.
26. **Yue S, Tang LY, Tang Y, Tang Y, Shen QH, Ding J, Chen Y, Zhang Z, Yu TT, Zhang YE, Cheng SY.** 2014. Requirement of Smurf-mediated endocytosis of Patched1 in Sonic Hedgehog signal reception. eLife **12:**e02555. http://dx.doi.org/10.7554/eLife.02555.
27. **Kay BK, Williamson MP, Sudol M.** 2000. The importance of being proline: the interaction of proline-rich motifs in signaling proteins with their cognate domains. FASEB J. **14:**231–241. http://dx.doi.org/10.1096/fj.1530-6860.

28. **Mouchantaf R, Azakir BA, McPherson PS, Millard SM, Wood SA, Angers A.** 2006. The ubiquitin ligase Itch is auto-ubiquitylated in vivo and in vitro but is protected from degradation by interacting with the deubiquitylating enzyme FAM/USP9X. J. Biol. Chem. **281:**38738–38747. http://dx.doi.org/10.1074/jbc.M605959200.
29. **Lu X, Liu S, Kornberg TB.** 2006. The C-terminal tail of the Hedgehog receptor Patched regulates both localization and turnover. Genes Dev. **20:**2539–2551. http://dx.doi.org/10.1101/gad.1461306.
30. **Bailey EC, Milenkovic L, Scott MP, Collawn JF, Johnson RL.** 2002. Several Patched1 missense mutations display activity in Patched1-deficient fibroblasts. J. Biol. Chem. **277:**33632–33640. http://dx.doi.org/10.1074/jbc.M202203200.
31. **Di Marcotullio L, Ferretti E, Greco A, De Smaele E, Po A, Sico MA, Alimandi M, Giannini G, Maroder M, Screpanti I, Gulino A.** 2006. Numb is a suppressor of Hedgehog signalling and targets Gli1 for Itch-dependent ubiquitination. Nat. Cell Biol. **8:**1415–1423. http://dx.doi.org/10.1038/ncb1510.
32. **Fombonne J, Bissey PA, Guix C, Sadoul R, Thibert C, Mehlen P.** 2012. Patched dependence receptor triggers apoptosis through ubiquitination of caspase-9. Proc. Natl. Acad. Sci. U. S. A. **109:**10510–10515. http://dx.doi.org/10.1073/pnas.1200094109.
33. **Rohatgi R, Milenkovic L, Scott MP.** 2007. Patched1 regulates Hedgehog signaling at the primary cilium. Science **317:**372–376. http://dx.doi.org/10.1126/science.1139740.
34. **Corbit KC, Aanstad P, Singla V, Norman AR, Stainier DY, Reiter JF.** 2005. Vertebrate Smoothened functions at the primary cilium. Nature **437:**1018–1021. http://dx.doi.org/10.1038/nature04117.
35. **Wang Y, Zhou Z, Walsh CT, McMahon AP.** 2009. Selective translocation of intracellular Smoothened to the primary cilium in response to Hedgehog pathway modulation. Proc. Natl. Acad. Sci. U. S. A. **106:**2623–2628. http://dx.doi.org/10.1073/pnas.0812110106.
36. **Molla-Herman A, Ghossoub R, Blisnick T, Meunier A, Serres C, Silbermann F, Emmerson C, Romeo K, Bourdoncle P, Schmitt A, Saunier S, Spassky N, Bastin P, Benmerah A.** 2010. The ciliary pocket: an endocytic membrane domain at the base of primary and motile cilia. J. Cell Sci. **123:**1785–1795. http://dx.doi.org/10.1242/jcs.059519.
37. **Li S, Chen Y, Shi Q, Yue T, Wang B, Jiang J.** 2012. Hedgehog-regulated ubiquitination controls Smoothened trafficking and cell surface expression in Drosophila. PLoS Biol. **10:**e1001239. http://dx.doi.org/10.1371/journal.pbio.1001239.
38. **Xia R, Jia H, Fan J, Liu Y, Jia J.** 2012. Usp8 promotes Smoothened signaling by preventing its ubiquitination and changing its subcellular localization. PLoS Biol. **10:**e1001238. http://dx.doi.org/10.1371/journal.pbio.1001238.
39. **Jimenez-Sanchez M, Menzies FM, Chang YY, Simecek N, Neufeld TP, Rubinsztein DC.** 2012. The Hedgehog signalling pathway regulates autophagy. Nat. Commun. **3:**1200. http://dx.doi.org/10.1038/ncomms2212.
40. **Huang S, Zhang Z, Zhang C, Lv X, Zheng X, Chen Z, Sun L, Wang H, Zhu Y, Zhang J, Yang S, Lu Y, Sun Q, Tao Y, Liu F, Zhao Y, Chen D.** 2013. Activation of Smurf E3 ligase promoted by smoothened regulates Hedgehog signaling through targeting Patched turnover. PLoS Biol. **11:**e1001721. http://dx.doi.org/10.1371/journal.pbio.1001721.
41. **Ingham RJ, Gish G, Pawson T.** 2004. The Nedd4 family of E3 ubiquitin ligases: functional diversity within a common modular architecture. Oncogene **23:**1972–1984. http://dx.doi.org/10.1038/sj.onc.1207436.
42. **Melino G, Gallagher E, Aqeilan RI, Knight R, Peschiaroli A, Rossi M, Scialpi F, Malatesta M, Zocchi L, Browne G, Ciechanover A, Bernassola F.** 2008. Itch: a HECT-type E3 ligase regulating immunity, skin and cancer. Cell Death Differ. **15:**1103–1112. http://dx.doi.org/10.1038/cdd.2008.60.